

<https://doi.org/10.48047/AFJBS.6.14.2024.5427-5439>



African Journal of Biological Sciences

Journal homepage: <http://www.afjbs.com>



Research Paper

Open Access

## Numerical study of a combined Photovoltaic thermal system using cellulose Nanocrystal (CNC) Nano-fluid

Ahmad Abdul Kareem Ahmad Aqeel<sup>1</sup>, Sami Hajjaj<sup>2</sup>, Hassan Mohamed<sup>3</sup>, Faten Saeed Obeidat<sup>4</sup>

<sup>1</sup> Institute of Informatics and Computing in Energy (IICE),

Universiti Tenaga Nasional (UNITEN), 43000, Kajang, Selangor, Malaysia

<sup>2</sup> Xi'an Jiaotong-Liverpool University, School of Robotics, 111 Taicang Avenue, Taicang, Suzhou, Jiangsu Province, 215400 P. R. China

<sup>3</sup> Institute of Sustainable Energy (ISE), Universiti Tenaga Nasional (UNITEN), 43000 Kajang, Selangor, Malaysia

<sup>5</sup> Department of Hearing and Speech Sciences, School of Rehabilitation Sciences, University of Jordan. Amman, 11942, Jordan

Eng\_shurman@yahoo.com, Sami.Hajjaj@xjtlu.edu.cn, mhassan@uniten.edu.my, faten.obeidat@ju.edu.jo

Volume 6, Issue 14, Aug 2024

Received: 15 June 2024

Accepted: 25 July 2024

Published: 15 Aug 2024

[doi:10.48047/AFJBS.6.14.2024.5427-5439](https://doi.org/10.48047/AFJBS.6.14.2024.5427-5439)

**Abstract.** This study examines the operational dynamics of a Photovoltaic/Thermal (PV/T) system, focused on simultaneous thermal and electrical energy generation under various conditions. The study covers PV/T system details, numerical modelling analysis and evaluates thermal and electrical output using Cellulose Nanocrystal (CNC) Nano-fluid. The main goal is to enhance PV system performance and reduce electricity generation costs. As the electrical output of the system is profoundly influenced by the operating temperature of PV cells, the integration CNC Nano-fluid is tested as a coolant to enhance PV cells' temperature control and system efficiency. The distinctive feature of this system lies in its capacity to augment electrical energy production while ameliorating solar radiation exposure, effecting PV module cooling, and engendering recoverable thermal energy for residential applications. Through the examination of the proposed system, it is ascertained that the zenith of energy output, encompassing both electrical and thermal facets, is achieved at a solar radiation intensity of 1000W/m<sup>2</sup> and a cooling fluid flow rate of 1.3 Kg/min, yielding 155W and 448W, respectively, with an attendant electrical efficiency of 17.1%. In contrast, an un-cooled PV module registers an electrical power generation of 142W, accompanied by an efficiency of 15.75%.

**Keywords:** Photovoltaic (PV), cooling system, efficiency, cellulose Nano crystal (CNC)

## 1 Introduction

Research and applications have focused on converting solar energy into electricity through photovoltaics (PV). This technology primarily converts solar radiation into electrical energy [1]. Specific physical processes limit a cell's efficiency; some are inherent and cannot be changed; many can improve by good design[2]. There are procedures that may be used to improve cell performance, such as cooling and concentration. PV mono-crystalline and multi-crystalline PV cells are the most commercial and efficient types made from silicon. However, it is also one of the costliest cells. Its efficiency is around 18%, depending on how much radiation is converted to energy, see fig 1.

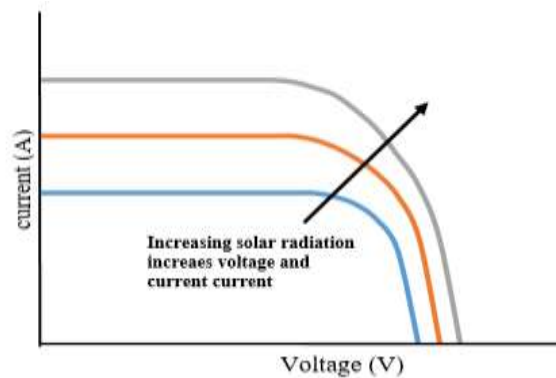


**Fig. 1.** A family of I-V curves for a solar cell [3], [4].

PV cells can reach temperatures up to 50 degrees Celsius above the ambient temperature [5], [6]. As the solar cell's temperature rises, the maximum power output drops, see Fig. (2). The ratio of conversion depends on the quality of materials used in the manufacture of PV cells and on their operating conditions.

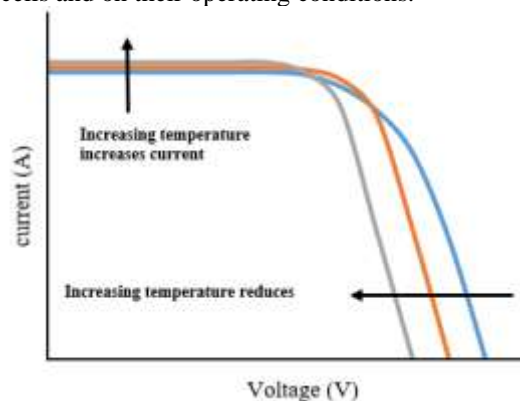


**Fig. 2.** Effect of temperature on the I-V characteristic [7].

The high temperature of the cells reduces their efficiency significantly. Numerous approaches to cooling photovoltaic (PV) modules, including the implementation of a PV/T air-heating manifold, have been presented in the literature [8], [9]. A hybrid solar system comprises a cooling mechanism linked to a solar PV panel, resulting in the generation of both electrical and thermal energy. This dual energy output can be harnessed to elevate the temperature of the cooling medium [10].

Nano-fluid is the most promising and recent approach to increase the efficiency of the PVT system, which consists of the dispersion of nanoparticles in base fluids. They contain unique physicochemical, optical, and biological features that may be tailored to the application [11]– [13]. Researchers have been studying the efficiency of solar panels utilizing nano-fluids as working fluids instead of traditional fluids for the past several years; Regrettably, researchers have observed that the utilization of nano-materials presents substantial concerns regarding their toxicity and safety implications [14]. Cellulose Nano Crystal (CNC) has garnered substantial interest from both industry and the academic community owing to its distinctive attributes. These attributes encompass cost-effectiveness, sourcing from renewable resources, low levels of toxicity, biodegradability, and remarkable mechanical properties [15]. Nano cellulose is an excellent material for creating high-performance nanocomposites. [16], [17].

Water and ethylene glycol have been used as a basis for much nano-fluid research because it reduces water's freezing point. Their low volatility is one of the key reasons they are suited for use as a thermal fluid in various conditions [18]. Nano-fluids can improve heat transmission and other features such as mass transfer. Dispersing nano cellulose in EGW produces a highly stable nano-fluid [19], [20].

This research looks at how nano-fluids might increase the efficiency of PV solar panels. CNC Nano-fluid will be used in PVT in this project to see if it can improve its efficiency in the steady state under the effect of solar radiation, also estimate the electrical and thermal energy, as well as the temperature of the PV cells and the temperature of the heat absorbers with changes in solar sunlight and the amount of cooling material flow.

## **2 Mathematical models of the PV/T collector**

Based on the findings of the previous studies, a home-based PV system that is simple to install and maintain, operates more effectively than conventional systems, and uses relatively inexpensive and readily accessible components has been developed. The total efficiency of the system presented in Fig. 3, which comprises a mono-crystalline PV panel cooled by CNC nano-fluid passing via copper pipes connected to its bottom surfaces, was recommended to be investigated.

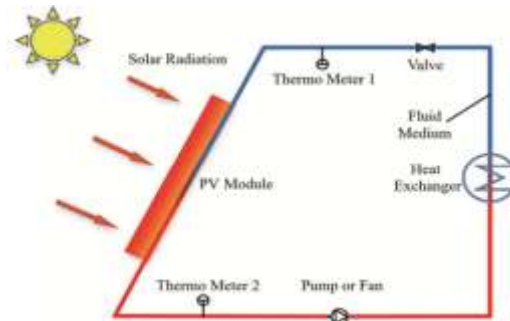


**Fig. 3.** Principal diagram of fluid medium cooling PV modules.

The base working fluids have been chosen to be water (W) with ethylene glycol (EG) (W: EG 60: 40 ratio). This is due to the nanoparticles' stability in the water-EG mix, and the 0.5 percent CNC volume concentration nano-fluid was chosen since it has the best stability and viscosity. As a result of the dispersion of nanocellulose in EGW, a very stable and high thermal conductivity nano-fluid is produced, which meets the needs of thermal applications, crystalline cellulose (CNC) nanoparticles with an 8.0% weight concentration were utilized according to Blue Goose Biorefiners Inc.'s requirements. The manufacturer has given CNC nanoparticle specs, as shown in Table 1 [20], [21].

**Table 1.** CNC specification parameters (Blue Goose Biorefineries Inc., n.d.).

Parameter	Value
Crystallinity index	80%
Crystal length	100-150 nm
Crystal diameter	9-14 nm
Hydrodynamic diameter	150 nm

The following assumptions are used to compute the different components' energy balance of a PV/T coolant receiver: (1) steady-state condition system, (2) The temperature varies very little along the thickness of the material, (3) The heat capacity of solar cell materials, tedlar, and insulation has been ignored., and (4) The coolant flow is consistent.

Figures 4 (a and b) show the components of the receiver as well as the absorber element's length ( $dx$ ) linked to the pipe of coolant material. Figure 5 depicts the system's equivalent circuit of the thermal resistance. These resistances are computed and utilized to estimate the PV/T coolant collector efficiency and thermal parameters.

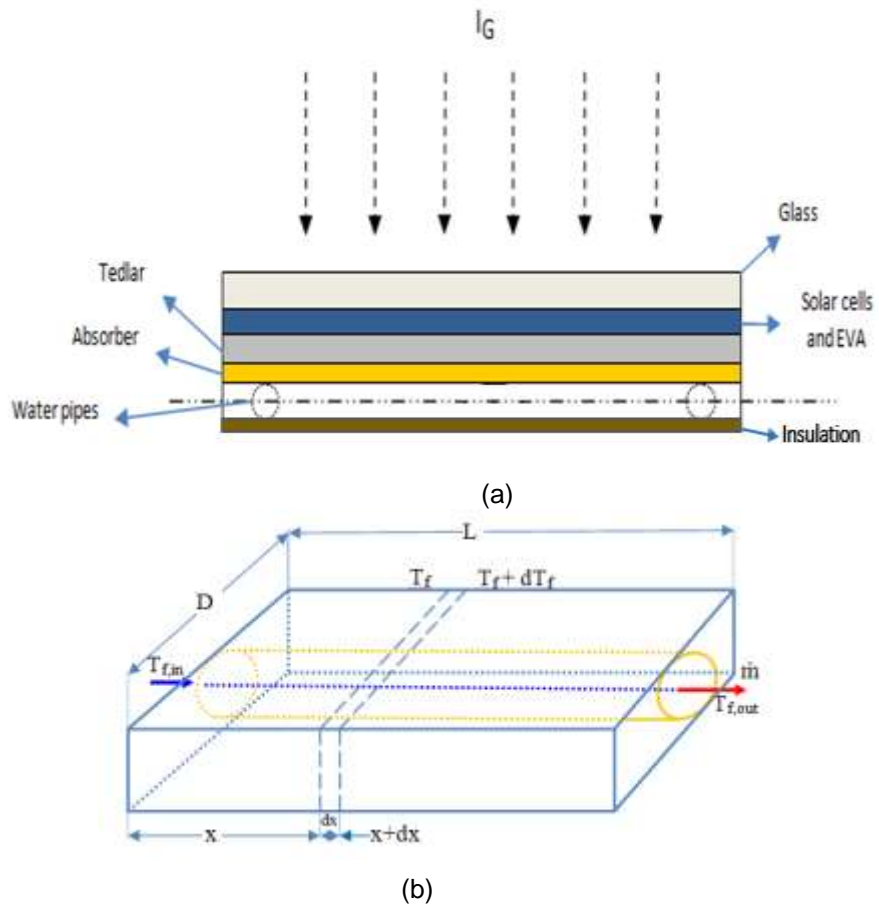


Fig. 4. (a) Module layers, (b) The absorber component's length (dx)

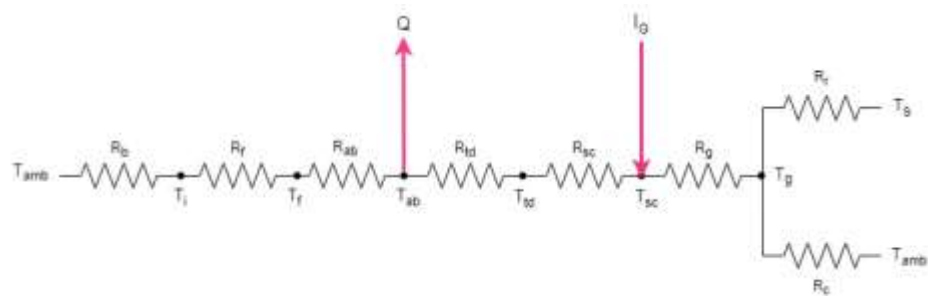


Fig. 5. The module's equivalent circuit for thermal resistance

After taking the glass-insulation component into account, energy balance equations for every part of the PV/T module were developed.

$$\tau_g [\alpha_{sc} \beta_{sc} I_G + \alpha_{td} (1 - \beta_{sc}) I_G] \cdot D \cdot dx = [U_{sc-amb} (T_{sc} - T_{amb}) + U_{sc-td} (T_{sc} - T_{td})] \cdot D \cdot dx + \tau_g \beta_{sc} \eta_{el} I_G \cdot D \cdot dx \tag{1}$$

Solar cells and tedlar absorb the solar energy rate available on the PV module equal to the summation of the total PV cell heat loss from the top surface to the surrounding plus the total PV cells heat transfer to the absorber face (back surface of the module where Ttd equal Tab) plus the rate of electrical energy produced. At the same time, the percentage of Tedlar plate area shielded from the sun by solar cells (packing factor) is represented by the symbol  $\beta_{sc}$ .

Where the symbols I, U, T, and D stand for solar radiation (W/m<sup>2</sup>), heat-transfer coefficient (W/m<sup>2</sup>K), temperature (K), and absorber width (m), while the Greek characters  $\tau$ ,  $\alpha$ ,  $\eta$  stand for transmissivity (-), absorptivity (-), and efficiency, respectively. Furthermore, in that sequence, the Subscripts Symbols g, sc, td, G, amb, and el stand for glass, solar cell, Tedlar, total, ambient, and electrical.

Finally, as an outcome of the rear surface (Absorber), the predicted solar cell temperature is derived as follows:

$$T_{sc} = [(\tau\alpha)_{eff} I_G + U_{sc-amb} T_{amb} + U_{sc-td} T_{td}] / (U_{sc-td} + U_{sc-amb}) \tag{2}$$

Moreover, the predicted back surface temperatures are as follows:

$$T_{ab} = [h_{p1} (\tau\alpha)_{eff} I_G + U_T T_{amb} + U_f T_{f,av}] / (U_f + U_T) \tag{3}$$

The temperature of the output cooling material Tf, out (K), and the quantity of usable heat transmitted to the heat removal agent, coolant, are calculated using Eqs. 3 and 4. [22].

$$T_{f,out} = \left( T_{amb} + \frac{h_{p1} h_{p2} [(\tau\alpha)_{eff} I_G]}{U_L} \right) \left( 1 - \exp \left( - \frac{F' U_L (D \cdot L)}{\dot{m} \cdot C_p} \right) \right) + T_{f,in} \cdot \exp \left( - \frac{F' U_L (D \cdot L)}{\dot{m} \cdot C_p} \right) \tag{4}$$

Where the symbols L,  $\dot{m}$ , CP, and F' stand for the length of absorber (m), mass flow rate (L/s), specific heat capacity (kJ/kg.K), and collector efficiency factor, respectively, while the Subscripts Symbols L, eff, f, in stand for overall, effectiveness and intake fluid in that sequence.

$$Q_u = F_R \cdot (L \cdot D) [h_{p1} h_{p2} \cdot [(\tau\alpha)_{eff} I_G] - U_L (T_{f,in} - T_{amb})] \tag{5}$$

where  $F_R$  stands for the heat removal efficiency factor and may be found at;

$$F_R = \frac{\dot{m} C_p}{U_L \cdot (L \cdot D)} \left[ 1 - \exp \left( - \frac{F' U_L (L \cdot D)}{\dot{m} C_p} \right) \right] \tag{6}$$

The thermal efficiency is calculated as follows:

$$\eta_{th} = \frac{Q_u}{[I_G \cdot A]} = \frac{Q_u}{[I_G (L \cdot D)]} = \frac{F_R}{I_G} [h_{p1} h_{p2} \cdot [(\tau\alpha)_{eff} I_G] - U_L (T_{f,in} - T_{amb})] = F_R [h_{p1} h_{p2} (\tau\alpha)_{eff} - (U_L / I_G) (T_{f,in} - T_{amb})] \tag{7}$$

Lastly, Eq. 8 produced the usable water heat transfer, which is shown as;

$$Q_u = F_R \cdot (L \cdot D) [h_{p1} h_{p2} \cdot [(\tau\alpha)_{eff} I_G] - U_L (T_{f,in} - T_{amb})] \quad (8)$$

The following equations were used to compute the PV module's electrical efficiency ( $\eta_{el}$ ) [23] and electrical power ( $P_{el}$ ) [24].

$$\eta_{el} = \eta_{el,r} [1 - \mu_{sc} (T_{sc} - T_{ref})] \quad (9)$$

$$P_{el} = \eta_{el} * I_G * D * L \quad (10)$$

Where  $\eta_{el,r}$  is a solar cell efficiency reference at 1000 W/m<sup>2</sup> solar irradiation,  $\mu_{sc}$  is the percent of electrical efficiency loss as a function of temperature ( $\mu_{sc}= 0.005$ ) and temperature  $T_{ref} = 298$  K.

The system's combined PV/T efficiency is the total of its thermal and electrical efficiencies, as follows:

$$\eta_{total} = \eta_{th} + \eta_{el} \quad (11)$$

Where  $\eta_{total}$  is the combined PV/T system's overall efficiency.

### 3 Results and discussion

When the quantity of solar radiation is changed from 200 to 1000 W/m<sup>2</sup>, and the cooling material flow rate volume is changed from (0.1 to 1.3) L/min, the PV system's performance improves. The average wind speed in this study was 1 m/s, and the cooling material temperature within the tank was 25 oC.

The electrical power of this system is illustrated in Fig. 6 under the impact of solar irradiance ranging from 200 to 1000 W/m<sup>2</sup>, indicating that the system's energy generated grows as the amount of solar radiation collecting increases. The most excellent quantity of energy was created at 1.3 Kg/min flow rate. The maximum amount of electric power generated rose from 32 W with solar radiation of 200 W/m<sup>2</sup> to 155 W with solar radiation of 1000 W/m<sup>2</sup>.

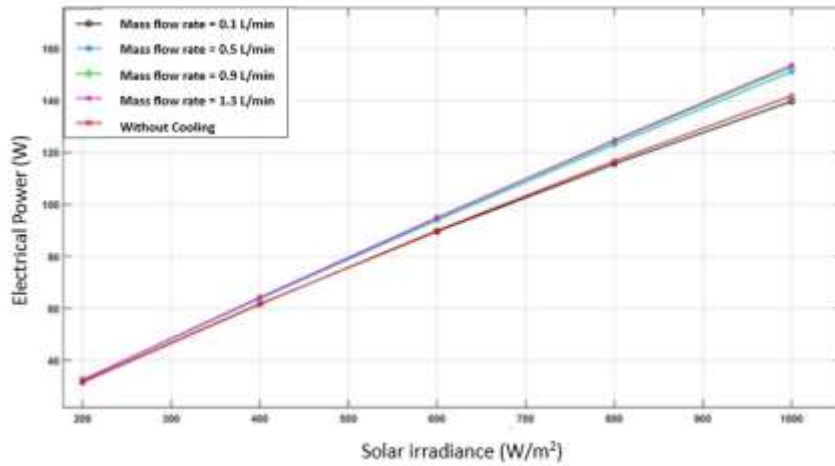


Fig. 6. Electric power vs. solar radiation for various amounts of cooling flow rate

Figures 7 and 8 demonstrate how the temperature of the solar cells and the heat absorber fluctuate as the number of solar radiation changes. Changes in the temperature of the solar cells are connected to changes in the heat absorber's temperature. They rise in tandem with rising solar radiation and fall in tandem with falling solar radiation. As indicated, cooling reduces the temperature of the solar cells and absorbers. When the coolant flow is low, the solar cells heat up more. Under solar irradiation of 1000 W/m<sup>2</sup> and a flow rate of 1.3 L/min, the temperature of the solar cells may reach 326 K, while the absorber temperature can reach 318 K under the same operating circumstances.

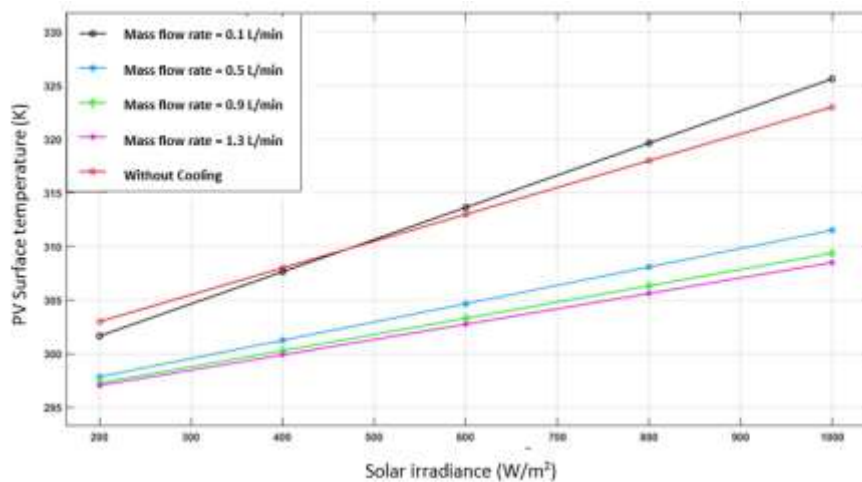
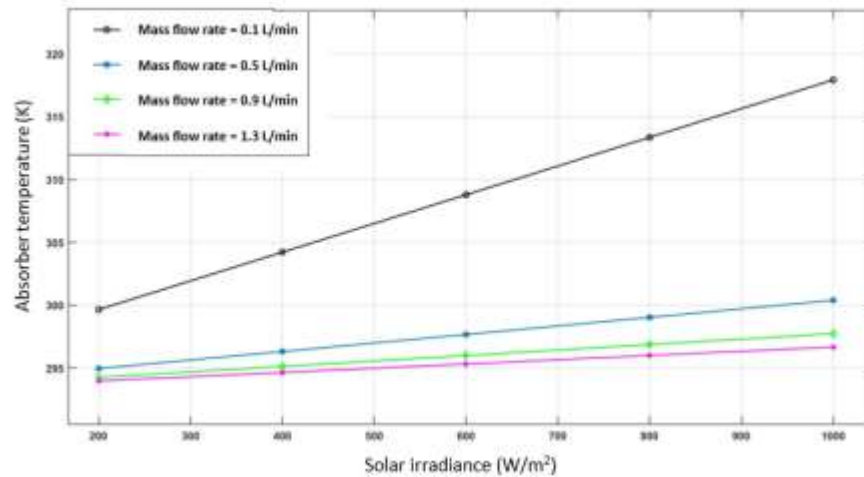


Fig. 7. Temperature of solar cells vs. solar radiation at various cooling flow rates





**Fig. 8.** Temperature of Absorber plate vs. solar radiation at various cooling flow rates

The electrical system efficiency under the same running situations is given in Fig. 9, which demonstrates that solar irradiance harms electrical ability, as evidenced by the fact that the electrical efficiency can drop from 17.7% at solar radiation of 200W/m<sup>2</sup> and 0.1 L/min coolant rate to 15.55% at the same coolant flow rate and 1000W/m<sup>2</sup> solar radiation. The considerable drop in electrical efficiency may be mitigated by increasing the volume of cooling material; for example, increasing the flow to 0.9 Kg/min at sun rays of 1000 W/m<sup>2</sup> raises the electrical efficiency to 17.0%.

The same impression that can be seen in the electrical system efficiency can also be seen in its thermal efficiency, as shown in Figure 10, where increased solar radiation lowers thermal efficiency while increasing cooling water flow lowers the efficiency deficit. According to Figure 11, the best thermal efficiency is 66% when solar radiation is 200W/m<sup>2</sup> and the flow rate is 1.3 L/min. In comparison, the lowest thermal efficiency is 31% when solar radiation is 1000W/m<sup>2</sup>, and the flow rate is 0.1 L/min.

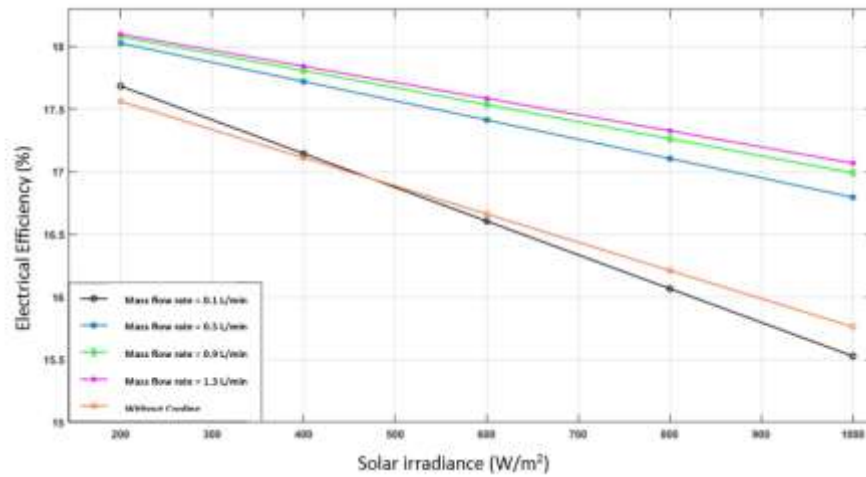


Fig. 9. Solar panel efficiency vs. solar radiation for various amounts of cooling flow rate

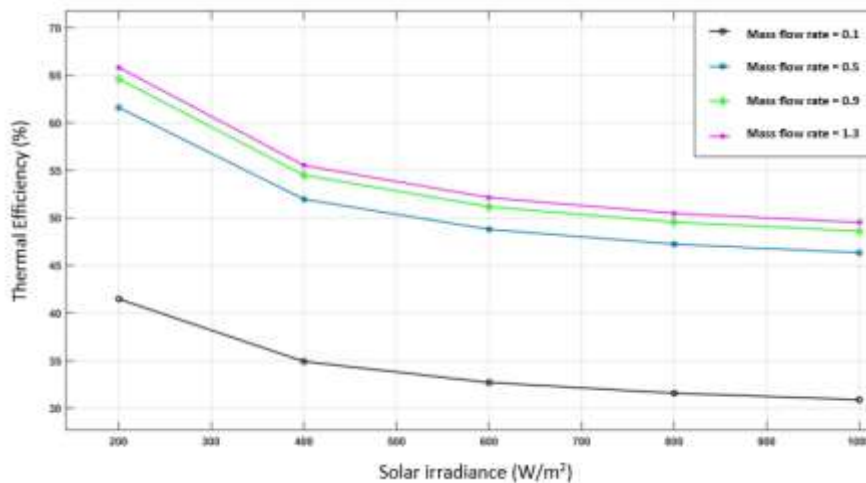
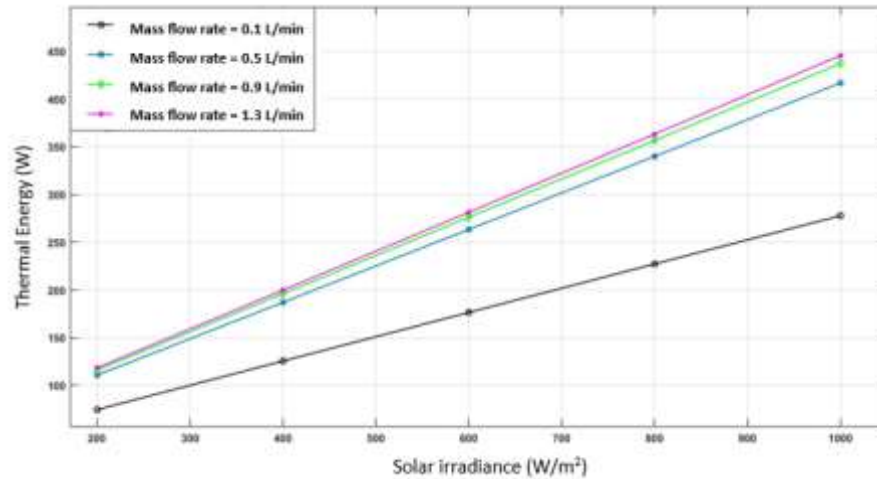


Fig. 10. Thermal efficiency vs. solar radiation for various amounts of cooling flow rate

The link between thermal energy and solar radiation is seen in Figure 11. When solar radiation increases and is accompanied by an increase in the flow rate of cooling material, the thermal energy generated increases significantly. The most significant quantity of thermal power was 448 W at 1000 W/m<sup>2</sup> and 1.3 L/min flow rate, while the lowest thermal energy quantity at 200 W/m<sup>2</sup> with the same coolant flow rate was 120 W.



**Fig. 11.** Thermal energy vs. solar radiation for varied amounts of cooling flow

After looking at several variables that affect the efficiency of the suggested solar system, it was found that electrical and thermal efficiency decreases as radiation from the sun increases. In contrast, electrical and thermal power, the temp of photovoltaics, and temp of solar collectors increase as solar radiation increases. With increasing the cooling material volume flow, the temp of photovoltaics and temp of solar collector decrease but thermal and electrical power increases.

#### 4 Conclusion

A mathematical examination of a PV/T was provided in this work; in this modeling, photovoltaic cells that are cooled by a significant cooling material flow and consume a lot of sun irradiance perform better than photovoltaic cells that use low solar radiation and a small amount of coolant flow under the same operating conditions. The greatest electrical and thermal energy gained was 155W and 448W, respectively, during the system analysis of the findings, at solar radiation 1000W/m<sup>2</sup> and 1.3 L/min coolant flow rate, whereas the electrical power provided by a PV module without cooling was 142W.

Increased sun radiation improves the performance of solar cells, but it also raises its temperature and the absorber temperature, lowering the electrical and thermal efficiency; increased cooling material via the collector enhances heat recovery from the PV module, resulting in higher electrical and thermal efficiency. Thus, in order to keep the temperature of the solar cells from rising to a point where they would lose their efficiency and become more vulnerable to damage, cooling is required for photovoltaic modules that employ strong solar radiation.

## References

- [1] E. P. Agbo, C. O. Edet, T. O. Magu, A. O. Njok, C. M. Ekpo, and H. Louis, "Solar energy: A panacea for the electricity generation crisis in Nigeria," *Heliyon*, vol. 7, no. 5. Elsevier Ltd, May 01, 2021. doi: 10.1016/j.heliyon.2021.e07016.
- [2] M. Rai, L. H. Wong, and L. Etgar, "Effect of Perovskite Thickness on Electroluminescence and Solar Cell Conversion Efficiency," *J Phys Chem Lett*, vol. 11, no. 19, pp. 8189–8194, Oct. 2020, doi: 10.1021/acs.jpcllett.0c02363.
- [3] R. Szabo and A. Gontean, "Photovoltaic Cell and Module I-V Characteristic Approximation Using Bézier Curves," *Applied Sciences*, vol. 8, no. 5, p. 655, Apr. 2018, doi: 10.3390/app8050655.
- [4] Vasilis Fthenakis and Paul A Lynn, *Electricity from sunlight: photovoltaic-systems integration and sustainability*, Second edition. UK: John Wiley & Sons Ltd, 2018.
- [5] S. Joseph Paul, U. Kumar, and S. Jain, "Photovoltaic cells cooling techniques for energy efficiency optimization," *Mater Today Proc*, vol. 46, pp. 5458–5463, 2021, doi: 10.1016/j.matpr.2020.09.197.
- [6] N. Abbas et al., "Applications of nanofluids in photovoltaic thermal systems: A review of recent advances," *Physica A: Statistical Mechanics and its Applications*, vol. 536. Elsevier B.V., Dec. 15, 2019. doi: 10.1016/j.physa.2019.122513.
- [7] M. Libra, T. Petrik, V. Poulek, I. I. Tyukhov, and P. Kourim, "Changes in the Efficiency of Photovoltaic Energy Conversion in Temperature Range With Extreme Limits," *IEEE J Photovolt*, vol. 11, no. 6, pp. 1479–1484, Nov. 2021, doi: 10.1109/JPHOTOV.2021.3108484.
- [8] S. Yogesh, K. S. Bijjargi, and K. A. Shaikh, "Cooling Techniques for Photovoltaic Module for Improving its Conversion Efficiency: A Review," *International Journal of Mechanical Engineering and Technology*, vol. 7, no. 4, pp. 22–28, 2016.
- [9] S. S. H. Hajjaj, A. A. K. A. Aqeel, M. T. H. Sultan, F. S. Shahar, and A. U. M. Shah, "Review of Recent Efforts in Cooling Photovoltaic Panels (PVs) for Enhanced Performance and Better Impact on the Environment," *Nanomaterials*, vol. 12, no. 10, p. 1664, May 2022, doi: 10.3390/nano12101664.
- [10] C. Good, J. Chen, Y. Dai, and A. G. Hestnes, "Hybrid Photovoltaic-thermal Systems in Buildings – A Review," *Energy Procedia*, vol. 70, pp. 683–690, May 2015, doi: 10.1016/J.EGYPRO.2015.02.176.
- [11] K. Bashirnezhad, M. Ghavami, and A. A. A. Alrashed, "Experimental investigations of nanofluids convective heat transfer in different flow regimes: A review," *J Mol Liq*, vol. 244, pp. 309–321, Oct. 2017, doi: 10.1016/J.MOLLIQ.2017.09.012.
- [12] R. B. Ganvir, P. V. Walke, and V. M. Kriplani, "Heat transfer characteristics in nanofluid—A review," *Renewable and Sustainable Energy Reviews*, vol. 75, pp. 451–460, Aug. 2017, doi: 10.1016/j.rser.2016.11.010.
- [13] T. Hayat, T. Muhammad, A. Alsaedi, and M. S. Alhuthali, "Magnetohydrodynamic three-dimensional flow of viscoelastic nanofluid in the presence of nonlinear thermal radiation," *J Magn Magn Mater*, vol. 385, pp. 222–229, Jul. 2015, doi: 10.1016/j.jmmm.2015.02.046.
- [14] L. Yang, X. B. Luo, and S. L. Luo, "Assessment on Toxicity of Nanomaterials," *Nanomaterials for the Removal of Pollutants and Resource Reutilization*, pp. 273–292, Jan. 2019, doi: 10.1016/B978-0-12-814837-2.00009-3.

- [15] S. Ben Cheikh, R. Ben Cheikh, E. Cunha, P. E. Lopes, and M. C. Paiva, "Production of cellulose nanofibers from Alfa grass and application as reinforcement for polyvinyl alcohol," *Plastics, Rubber and Composites*, vol. 47, no. 7, pp. 297–305, Aug. 2018, doi: 10.1080/14658011.2018.1479822.
- [16] K. Ramachandran, K. Kadirgama, D. Ramasamy, W. H. Azmi, and F. Tarlochan, "Investigation on effective thermal conductivity and relative viscosity of cellulose nanocrystal as a nanofluidic thermal transport through a combined experimental – Statistical approach by using Response Surface Methodology," *Appl Therm Eng*, vol. 122, pp. 473–483, 2017, doi: 10.1016/j.applthermaleng.2017.04.049.
- [17] S. A. Razali, N. Azwadi, C. Sidik, and H. Koten, "Cellulose Nanocrystals: A Brief Review on Properties and General Applications," *Journal of Advanced Research Design Journal homepage*, vol. 60, pp. 1–15, 2019.
- [18] F. Benedict et al., "Nanocellulose as heat transfer liquid in heat exchanger," in *AIP Conference Proceedings*, American Institute of Physics Inc., Jan. 2019. doi: 10.1063/1.5085987.
- [19] K. Farhana, K. Kadirgama, M. M. Noor, M. M. Rahman, D. Ramasamy, and A. S. F. Mahamude, "CFD modelling of different properties of nanofluids in header and riser tube of flat plate solar collector," *IOP Conf Ser Mater Sci Eng*, vol. 469, p. 012041, Jan. 2019, doi: 10.1088/1757-899X/469/1/012041.
- [20] L. Samylingam et al., "Thermal analysis of cellulose nanocrystal-ethylene glycol nanofluid coolant," *Int J Heat Mass Transf*, vol. 127, pp. 173–181, Dec. 2018, doi: 10.1016/j.ijheatmasstransfer.2018.07.080.
- [21] I. Naiman Ibrahim, N. Sazali, D. Ramasamy, A. Shahir Jamaludin, M. Syafiq Sharip, and H. Ibrahim, "Effect of Impregnate Nanocellulose With Ethylene Glycol for Car Radiator Application," *Journal of Advanced Research in Fluid Mechanics and Thermal Sciences Journal homepage*, vol. 58, pp. 43–50, 2019.
- [22] M. A. Hasan and K. Sumathy, "Photovoltaic thermal module concepts and their performance analysis: A review," *Renewable and Sustainable Energy Reviews*, vol. 14, no. 7, pp. 1845–1859, Sep. 2010, doi: 10.1016/j.rser.2010.03.011.
- [23] E. Venegas-Reyes, N. Ortega-Avila, M. I. Peña-Cruz, O. J. García-Ortiz, and N. A. Rodríguez-Muñoz, "A Linear Hybrid Concentrated Photovoltaic Solar Collector: A Methodology Proposal of Optical and Thermal Analysis," *Energies (Basel)*, vol. 14, no. 23, p. 8155, Dec. 2021, doi: 10.3390/en14238155.
- [24] H. M. S. Bahaidarah, "Experimental performance evaluation and modeling of jet impingement cooling for thermal management of photovoltaics," *Solar Energy*, vol. 135, pp. 605–617, Oct. 2016, doi: 10.1016/J.SOLENER.2016.06.015.